Transmission electron microscopy study of $In_xGa_{1-x}As$ quantum dots on a GaAs(001) substrate

J. Zou,* X. Z. Liao, and D. J. H. Cockayne
Australian Key Centre for Microscopy and Microanalysis, The University of Sydney, NSW 2006, Australia

R. Leon†
Department of Electronic Materials Engineering, Research School of Physical Sciences and Engineering, Australian National University, Canberra, ACT 0200, Australia

(Received 30 June 1998; revised manuscript received 2 November 1998)

A transmission electron microscopy (TEM) investigation of the morphology of $In_xGa_{1-x}As$ quantum dots grown on a GaAs(001) substrate has been carried out. The size and the shape of the quantum dots have been determined using bright-field images of cross-section TEM specimens and [001] on-zone bright-field images with imaging simulation from plan-view TEM specimens. The results suggest that the coherent quantum dots are lens shaped with base diameters of 25–40 nm and aspect ratios of height to diameter of 1:6–1:4. [S0163-1829(99)00920-0]

Since Esaki and Tsu[1] proposed the idea of semiconductor heterostructures and successfully grew $Al_xGa_{1-x}As$/GaAs superlattices nearly three decades ago, quantum semiconductor structures have received increasing attention due to their potential applications in electronic and optoelectronic devices and circuits.[2,3] In recent years, fabrication of low-dimensional quantum semiconductor structures, such as quantum wires and quantum dots, has become possible with the development of modern epitaxial techniques. Compared with bulk or quantum well systems, these low-dimensional quantum semiconductor structures have unique and superior optical properties for optoelectronic devices. For quantum dots, carriers are confined three dimensionally, leading to different optoelectronic properties from those in bulk materials, quantum wells, and quantum wires. Since the shape and size of quantum dots are critical parameters in determining their optoelectronic properties,[4–7] determination of these parameters is important. Several techniques have been used to estimate these parameters, such as atomic force microscopy (AFM),[8–14] scanning tunneling microscopy,[15–17] reflection high-energy electron diffraction,[18,19] and transmission electron microscopy (TEM).[20–24] Different shapes of quantum dots such as lens-shaped,[9,10,23] cone-shaped,[14,17] pyramids with different facets,[11,12,18–21] and truncated pyramids[22] have been reported using the above techniques. Differences in the predicted values for quantum dot ground state and excited state emission, and in intersublevel energies will be obtained depending on what shapes and aspect ratios are assumed in the calculation. Calculations for both pyramid-shaped[25,26] and lens-shaped $In_xGa_{1-x}As$/GaAs quantum dots[27] have been reported; however, an exact experimental determination of the shape of these islands is at present controversial. AFM has been the most commonly used technique for the shape and size study of uncapped quantum dots. However, the convolution of the AFM tip with the dot structure limits its ability to resolve the shape of very small quantum dots,[28,29] and especially of the dots with facets. Although TEM techniques have been used to study the shape and size of the dots, reliable information has not been obtained. In this study, a comprehensive TEM investigation of the shape and the size of uncapped $In_xGa_{1-x}As$ quantum dots grown on GaAs(001) is carried out.

The $In_{0.6}Ga_{0.4}As$ quantum dots were grown on a GaAs(001) substrate by metalorganic chemical-vapor deposition using a horizontal reactor cell operating at 76 Torr. For the growth of $In_xGa_{1-x}As$ islands, $(CH_3)_3Ga_3$, $(CH_3)_3In$, and AsH_3 were used as precursors. The flow of $(CH_3)_3In$ was monitored and controlled by an EPISON ultrasonic sensor. The H_2 carrier flow rate was 17.5 standard litres per minute. After growth of a 200-nm GaAs buffer layer at 650 °C, the temperature was lowered to 590 °C and nanometer-sized $In_xGa_{1-x}As$ islands were grown by depositing 5 ML of $In_{0.6}Ga_{0.4}As$. Growth rates were nominally 0.5 ML per second.

$\langle 110 \rangle$ cross section and [001] plan-view TEM specimens were prepared by mechanical thinning and dimple grinding, and followed by ion-beam thinning using a Gatan 660 Ion-Beam Thinner with a cold stage to prevent preferred thinning. These specimens were examined in Philips EM430 and Philips CM12 transmission electron microscopes operating at 300 and 120 kV, respectively.

Side projections of quantum dots were studied using cross-section TEM specimens. Since the edge of a quantum dot is very thin from the TEM specimen point of view, TEM images must be taken in the under defocus condition to make the edge of the dots distinct, and consequently to be able to measure the dimension of the quantum dots. Figure 1 is a

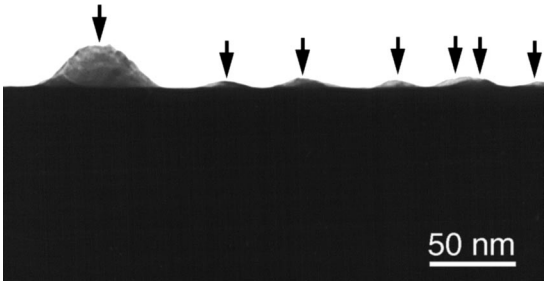

FIG. 1. A bright-field image of a cross-section TEM specimen showing a side projection of quantum dots (arrowed).

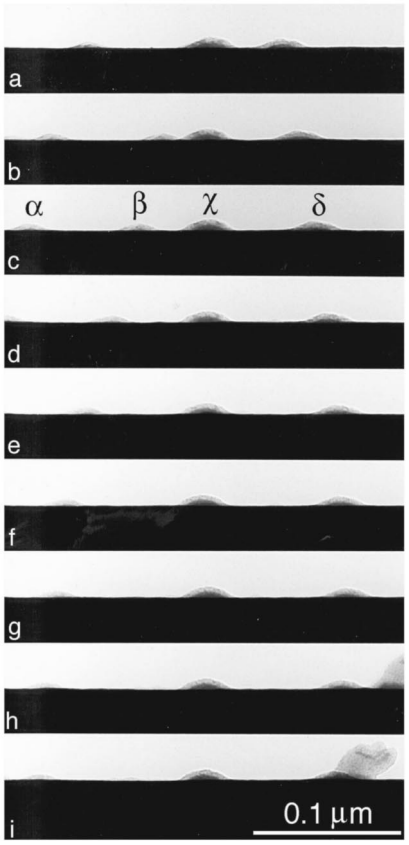

FIG. 2. A series of bright-field images obtained by tilting the TEM specimen along the [001] axis. The quantum dots χ has been put into the center of the image to carry out a detailed analysis.

bright-field image showing a typical example of the quantum dots. The image suggests that the projection of the small quantum dots is arc shaped while the large dot is trapezoidal in shape. Defining the dot projection adjacent to the flat surface as the base projection, investigation showed that most of the quantum dots have base projections varying between 25 and 40 nm. Larger quantum dots can be found occasionally with base projections up to 200 nm. Because the large quantum dots are relaxed, we concentrate our investigation on those quantum dots, which are coherent and have their base projection sizes varying between 25 and 40 nm.

Since Fig. 1 is only a side projection of the quantum dots, other projections are needed for the complete determination of their shape and size. To estimate the three-dimensional information of the quantum dots, a continuous tilting (up to 120°) experiment was carried out. To ensure that quantum dots would not be damaged during the TEM specimen preparation, the substrate region was chosen to be much thicker (>300 nm) than the dot dimension (~ 30 nm), in this way, the chance that quantum dots were cut in section was small. Because the surface normal of the sample is [001], the TEM specimen was tilted around [001] to ensure that the sample surface remained precisely parallel to the electron beam. Figure 2 is an example of the continuous tilting experiment with Figs. 2(a)–2(i) being taken at intervals of 10°. It is noted that, for each dot in Fig. 2, there is a semitransparent contrast layer surrounding the image. It has been proved that, by taking dark-field images using crystal reflections, this layer is crystalline and not amorphous. The appearance of the layer

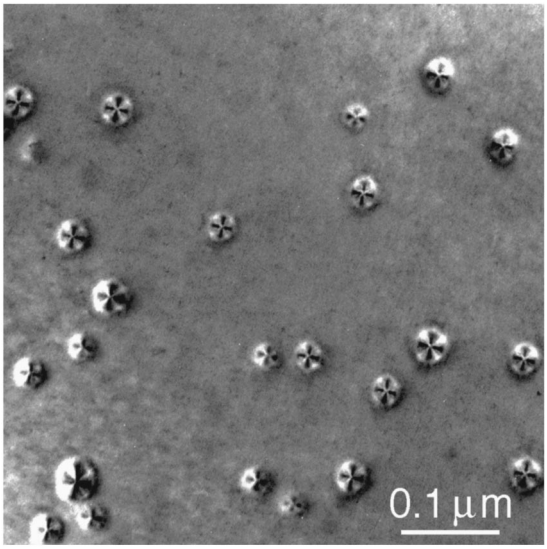

FIG. 3. A [001] on-zone bright-field image taken from a plan-view TEM specimen showing the contrasts of the quantum dots.

as being different from the rest of the quantum dot is, we believe, an artifact of the imaging, resulting from the geometry of the dot within the thin specimen. With the continuous change of tilting angle one sees the distance between the dots change continuously; but it is noted that the height of all these dots remains constant. There are four quantum dots in Fig. 2, marked α, β, χ, and δ. Careful analysis of the quantum dot marked χ shows that the base projections of the dot remain constant through the tilting range, indicating that the dot has a circular base. A similar result was observed for most of dots studied. Since the surface profile of the quantum dots in all cases are arc shaped, this implies that the dots have a lens profile with a flat circular base of diameter equal to the length of their base projections.

Although the technique outlined above can provide detailed information about the shape and size of quantum dots, only a limited number of quantum dots can be studied for each TEM specimen. To obtain better statistics, plan-view TEM specimens were investigated using the [001] on-zone bright-field imaging. Figure 3 is a typical example showing a large number of the quantum dots [an enlarged quantum dot is shown in Fig. 4(a)], in which two points are noted: (i) the contrast of each quantum dot has an approximately circular

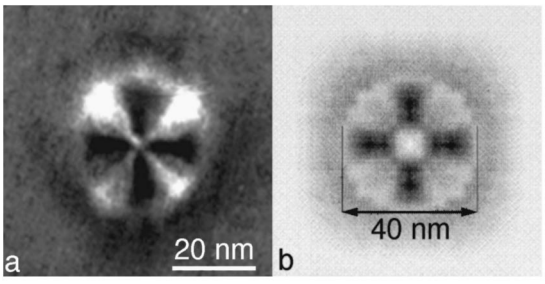

FIG. 4. (a) An enlarged on-zone bright-field image showing a quantum dot and (b) a simulated [001] on-zone bright-field image of an uncapped quantum dot with spherical cap shape. The following TEM parameters are used in the image simulation: 120 keV and 29 electron beams.

edge and (ii) some images of dots are slightly elliptical in shape, with axes different in length by up to 10%.

Since the contrast in a diffraction contrast image [such as Fig. 4(a)] arises from the strain field, care has to be taken if the contrast information is to be used to determine the size of the quantum dots. To determine the size of quantum dots from the image, image simulation was carried out. The strain field of a spherical cap-shaped quantum dot with base diameter of 40 nm and an aspect ratio of height to base diameter of 1:4 was modeled using finite element analysis (STRAND6 software[30]). The anisotropic elastic constants c_{11}, c_{12}, and c_{44} of $In_xGa_{1-x}As$ were set equal to those of GaAs to simplify the calculation.[31] The calculated strain distribution was used in a dynamical electron scattering program to generate simulated images. Figure 4(b) shows an example of a simulated [001] on-zone bright-field image. It is seen that the image of the quantum dot has a circular edge with fourfold symmetry inside the perimeter. These features are in excellent agreement with the observed quantum dots in on-zone bright-field images [see Fig. 4(a)]. Careful analysis from simulated images showed that the image contrast changes rapidly at the edge of the dot [see Fig. 4(b)], so that the image diameter can be use to estimate the size of the quantum dots. For this reason, we conclude that, for the uncapped $In_xGa_{1-x}As$ quantum dots grown on the (001) GaAs substrate, the on-zone bright-field imaging technique from plan-view TEM specimens can be used to determine the base diameters of the quantum dots. The calculation method and analysis of images is to be reported in detail in a future publication.

Combining the two TEM techniques, the shape and the size of the uncapped $In_xGa_{1-x}As$ quantum dots grown on the GaAs substrate can be obtained more accurately than has been possible previously. Studies of a number of quantum dots in these samples have shown that the dots are lens shaped with more than 90% of them having their base diameter in the range of 25–40 nm and with aspect ratios of height to base diameter of 1:4–1:6. Furthermore, detailed investigation showed that this range of aspect ratios applies to quantum dots having the same base diameter. For the most frequently observed quantum dots (with base diameters from 30 to 35 nm), their aspect ratios varied from 1:4 to 1:5, which agrees with the ratios measured by AFM and cross section high resolution electron microscopy for uncapped quantum dots.[3,15,21] The smaller quantum dots with base diameters around 25 nm have aspect ratios about 1:6. The larger quantum dots with base diameters around 40 nm have aspect ratios around 1:4. These results suggest a tendency for dots with larger base diameter to have larger aspect ratios. This tendency is consistent with the theoretical prediction of Johnson *et al.*[32] for Ge/Si quantum dots. In this study, the coverage of the quantum dots was determined to be around 6%.

In conclusion, the shape and size of uncapped $In_xGa_{1-x}As$ quantum dots grown on GaAs(001) has been unambiguously determined by using a continuous tilting experiment of cross-section TEM specimens combined with [001] on-zone bright-field imaging and image simulation. The quantum dots in this study have been shown to be lens shaped with a circular base. The aspect ratios of height to base diameter vary between 1:4–1:6 where the dots with larger base diameters tend to have larger aspect ratio.

The authors would like to thank the Australian Research Council for financial support, Professor S. Matsumura for providing an original simulation program, and Dr. G. Anstis for assistance with the programming. Sydney Regional Visualization Laboratory is acknowledged for facilities for the calculation of the strain distribution.

*Electronic address: zou@emu.usyd.edu.au

†Present address: Jet Propulsion Laboratory, California Institute of Technology, 4800 Oak Grove Drive, Pasadena, California 91109-8099.

[1] L. Esaki and R. Tsu, IBM J. Res. Dev. **14**, 61 (1970).

[2] G. C. Osbourn, IEEE J. Quantum Electron. **QE-22**, 1677 (1986).

[3] K. Nomoto, R. Ugajin, T. Suzuki, K. Taira, and I. Hase, IEICE Trans. Electron. **81**, 8 (1998).

[4] H. Jiang and J. Singh, Phys. Rev. B **56**, 4696 (1997).

[5] R. Leon, S. Fafard, D. Leonard, J. L. Merz, and P. M. Petroff, Appl. Phys. Lett. **67**, 521 (1995).

[6] A. A. Seraphin, E. Werwa, and K. D. Kolenbrander, J. Mater. Res. **12**, 3386 (1997).

[7] J. L. Zhu, Z. Q. Li, J. Z. Yu, K. Ohno, and Y. Kawazoe, Phys. Rev. B **55**, 15 819 (1997).

[8] C. Lobo and R. Leon, J. Appl. Phys. **83**, 4168 (1998).

[9] J. M. Moison, F. Houzay, F. Barthe, L. Leprince, E. Andre, and O. Vatel, Appl. Phys. Lett. **64**, 196 (1996).

[10] J. H. Zhu, K. Brunner, and G. Abstreiter, Appl. Phys. Lett. **72**, 424 (1998).

[11] H. Saito, K. Nishi, S. Sugou, and Y. Sugimoto, Appl. Phys. Lett. **71**, 590 (1997).

[12] Z. Zhu, E. Kurtz, K. Arai, Y. F. Chen, D. M. Bagnall, P. Tomashini, F. Lu, T. Sekiguchi, T. Yao, T. Yasuda, and Y. Segawa, Phys. Status Solidi B **202**, 827 (1997).

[13] D. Hommel, K. Leonardi, H. Heinke, H. Selke, K. Ohkawa, F. Gindele, and U. Woggon, Phys. Status Solidi B **202**, 835 (1997).

[14] Y. Hasegawa, T. Egawa, T. Jimbo, and M. Umeno, Appl. Phys. Lett. **68**, 523 (1996).

[15] Y.-W. Mo, D. E. Savage, B. S. Swartzentruber, and M. G. Lagally, Phys. Rev. Lett. **65**, 1020 (1990).

[16] W. Wu, J. R. Tucker, G. S. Solomon, and J. S. Harris, Jr., Appl. Phys. Lett. **71**, 1083 (1997).

[17] M. Horn-von Hoegen, A. Al Falou, B. H. Muller, U. Kohler, L. Andersohn, B. Dahlheimer, and M. Henzler, Phys. Rev. B **49**, 2637 (1994).

[18] H. Lee, R. Lowe-Webb, W. Yang, and P. C. Sercel, Appl. Phys. Lett. **72**, 812 (1998).

[19] Y. Nabetani, T. Ishikawa, S. Noda, and A. Sasaki, J. Appl. Phys. **76**, 347 (1994).

[20] S. Ruvimov, P. Werner, K. Scheerschmidt, U. Gosele, J. Heydenreich, U. Richter, N. N. Ledentsov, M. Grundmann, D. Bimberg, V. M. Ustinov, A. Yu. Egorov, P. S. Kop'ev, and Z. I. Alferov, Phys. Rev. B **51**, 14 766 (1995).

[21] K. Tillmann, A. Thust, M. Lentzen, P. Swiatek, A. Forster, K. Urban, W. Laufs, D. Gerthsen, T. Remmele, and A. Rosenauer, Philos. Mag. Lett. **74**, 309 (1996).

[22] K. Georgsson, N. Carlsson, L. Samuelson, W. Seifert, and L. R. Wallenberg, Appl. Phys. Lett. **67**, 2981 (1995).

[23] D. J. Eaglesham and M. Cerullo, Phys. Rev. Lett. **64**, 1943 (1990).

[24] X. Z. Liao, J. Zou, X. F. Duan, D. J. H. Cockayne, R. Leon, and C. Lobo, Phys. Rev. B **58**, R4235 (1998).
[25] M. Grundmann, O. Stier, and D. Bimberg, Phys. Rev. B **52**, 11 969 (1995).
[26] C. Pryor, Phys. Rev. B **57**, 7190 (1998).
[27] A. Wojs, P. Hawrylak, S. Fafard, and L. Jacak, Phys. Rev. B **54**, 5604 (1996).
[28] H. Lee, R. Lowe-Webb, W. Yang, and P. C. Sercel, Appl. Phys. Lett. **72**, 812 (1998).
[29] D. Leonard, K. Pond, and P. M. Petroff, Phys. Rev. B **50**, 11 687 (1994).
[30] http://www.strand.aust.com
[31] J. S. Blakemore, J. Appl. Phys. **53**, R123 (1982).
[32] H. T. Johnson and L. B. Freund, J. Appl. Phys. **81**, 6081 (1997).